Hydrothermally Fluorinated Graphene Oxide Chemiresistive Sensor for Detecting NH_3 and Acetone under Atmospheric Conditions

Ivan Amor, Bruno Gamero, Siziwe Bebe and Ravi Prakash*
Department of Electronics Engineering, Carleton University, Ottawa, Canada

Keywords: Biosensor, Health Monitoring, Electronic Sensor, Chemiresistor, Graphene Oxide, Exhaled Breath Detection, Multi-analyte Sensing.

Abstract: Emergence of graphene-derived highly functional materials has transformed chemical and bio sensing, with several novel approaches utilizing chemical modification of graphene oxide (GO). These materials have been implemented in device fabrication for the detection of biomolecules, volatile organic compounds (VOC), and other chemical analytes. The detection methods rely on using specificity of the modified graphene material to target selective and quantifiable electrical responses. In this work, we report ultra-low-level detection of NH_3 (1-10 ppm) and extend the same chemiresistor sensor to additionally detect acetone and distinguish between their individual transient responses. The low-level detection of both these gaseous analytes is highly relevant, and the comparable physiological detection range of these analytes makes the device suitable for continuous health monitoring and detecting specific gas molecules in exhaled breath. The sensor system is compactly designed to make it low cost and ideal for wearable health monitoring and environmental monitoring, using an in-house hydrothermal fluorination technique to synthesize fluorinated-GO (FGO) suspension, and its solution-phase deposition onto interdigitated chrome electrodes to create the chemiresistive gas sensor. The sensor device reported a highly linear detection range for NH_3, ranging over 1 – 10 ppm and was additionally able to detect acetone in a similar low concentration range, whilst distinguishing the two gases based on its rapid transient response.

1 INTRODUCTION

Chemiresistors, along with electrochemical sensors, are widely used as gas sensing devices, and for a variety of chemical sensing applications (Yadava et al., 2012; Sanchez et al., 2006; Lin et al., 2015). Electrochemical sensors adequately target metabolites and electrolytes through enzymatic, ion-selective, electroactive reactions (Zhao et al., 2020). However, there are several disadvantages to their implementation for non-invasive and continuous health applications (Gargiulo et al., 2020). Their dependence on elaborate patterning steps and temperature sensitivity results in higher complexity. Chemiresistors on the other hand, offer the benefit of sensing various analytes due to the configurable layer properties of the sensor. In addition, chemiresistive sensors are simpler to fabricate, require less operating power, and possess a longer operational life span than electrochemical detectors (Sanchez et al., 2006; Lin et al., 2015; Zampolli et al., 2007). They prove to be excellent candidates for ultra-low molecular concentration detection in a non-invasive, continuous health care monitoring approach, to potentially observe and indicate important physiological conditions by identifying target gaseous analytes (Majumder et al., 2017). Chemiresistors are commonly implemented using metal oxide (MOx) sensitive films such as tin or titanium oxide and require high temperature for gas detection (Wang et al., 2010; Ponzoni et al., 2017). This is achieved using a thermistor integrated into the device, or a sensing layer is deposited on a micro-hot plate for optimal operating temperature (Lin et al., 2015; Manginell et al., 1997).

Graphene has attracted great attention among available 2-D materials for both chemical sensing applications. Its morphological characteristics, especially its high surface to volume ratio has been attractive for gas sensing applications. Graphene contains high electronic charge mobility, Young's modulus, and thermal conductivity, which makes it an ideal candidate material for integrated circuitry, energy storage, and chemical and bio-electronic

Amor, I., Gamero, B., Bebe, S. and Prakash, R.
Hydrothermally Fluorinated Graphene Oxide Chemiresistive Sensor for Detecting NH3 and Acetone under Atmospheric Conditions.
DOI: 10.5220/0010241200990106
In *Proceedings of the 14th International Joint Conference on Biomedical Engineering Systems and Technologies (BIOSTEC 2021) - Volume 1: BIODEVICES*, pages 99-106
ISBN: 978-989-758-490-9

sensors. During the oxidation process of graphene, sp^3 bonding is heavily interrupted and makes electrical conductivity of graphene oxide (GO) decrease drastically compared to pristine graphene (Zaaba et al., 2017). GO can be modified to produce functionalized GO (FGO), which has lower or higher conductivity properties than pristine graphene and GO (Huang et al., 2011; Kavinkumar et al., 2015). This makes FGO a suitable candidate for replacing MOx in chemiresistors. Another benefit is that FGO can be produced using cost-effective chemical methods, and in high yields from the inexpensive graphite raw material. In addition, due to its hydrophilic nature, stable aqueous colloids can be formed to facilitate the assembly of macroscopic structures by simple, low-cost solution deposition processes (Park et al., 2016; Chronopoulos et al., 2017). Reducing graphene oxide by fluorination offers several advantages, owing to the low polarity of C–F bonds and the high polarity of oxygenic groups, characteristics of FGO could be tuned by controlling the C–F and C–O ratios. Oxygen or fluorine atom concentration can be tuned for different end-product usage (Karlický et al., 2013). The main advantage of FGO for sensing is its high electrocatalytic activity (augmented electron transfer), and specificity toward certain analytes due to the presence of C–F bonds (Urbanova et al., 2016; Lu et al., 2009). It has been observed that low fluorinated graphene exhibits excellent sensing properties for a range of studied biomolecules - including ionized (NH4+), unionized ammonia (NH_3), and gaseous NH_3, nicotinamide adenine dinucleotide (NADH), ascorbic acid (AA), uric acid (UA), and dopamine (DA). The low fluoride (F) content that augments the electron transfer from electrode to biomolecule (or vice versa) will neither significantly affect the electrical conductivity nor the wetting properties of graphene (Zhu et al., 2019; Huang et al., 2012). Exploration of ammonia sensing using graphene-based platforms is rapidly evolving (Huang et al., 2012; Schedin et al., 2007). Recent Discrete Fourier Transform (DFT) studies by Yeon Hoo Kim et al. predicted that the binding of GO with NH_3 molecules can be enhanced by decreasing electron density of GO (Kim et al., 2017).

In this work, we have demonstrated a small footprint, low-cost, FGO based chemiresistive gas sensor, implemented on a variety of substrate materials, for rapid and ultra-low concentration detection of NH_3 (~ 1 – 10 ppm). The operating principle of our chemiresistive sensor relies on adsorption of gas molecules in a sensitive 2-D film and the resultant change in electrical resistance (Manginell et al., 1997; Bârsan et al., 1995; Zhao et al., 2019; Briand et al., 2000). In our approach, a layer of chemically functionalized graphene oxide thin film material was deposited onto the interdigitated metal electrodes. To render the graphene oxide selective to target gas molecules, functional groups were added through chemical modification. We furthermore investigated detection of Acetone to establish the multi-analyte sensing capability of our system. We chose ammonia as the target analyte due to its importance in diverse biological processes. Commercial sensors exist for detecting ammonia in ranges above 10 ppm, but they are not adequately sensitive for healthcare centric applications. Samples of ammonia that are discharged from the body are used to monitor systemic ammonia levels (Gafare et al., 2014). Multi analyte detection of acetone is also crucial for monitoring conditions such as diabetes. Studies have shown that persons with diabetes would exhibit an ultra-low concentration of acetone (> 1.8ppm) in exhaled breath (Xiao et al., 2014).

2 MATERIALS AND METHODS

XtalFluor-E (XtalFluor), hydrofluoric acid (HF), sodium hydrogen carbonate, poly-(3,4-ethylenedioxythiophene polystyrene sulfonate (PEDOT:PSS), polyvinyl alcohol (PVA) and poly-methyl methacrylate (PMMA) were acquired from Sigma Aldrich. De-ionized water was gathered from the local micro fabrication lab on-site regeneration system.

A specialized Teflon beaker with a specially formulated stabilized poly-tetrafluoro ethylene (PTFE) carbon base to aid in heating was obtained from Canada wide Scientific (Dynalon Labware) for the synthesis process.

Surface oxidized (passivated) silicon (pSi) and silicon (Si) substrates with chromium Interdigitated Electrodes (IDEs) were fabricated at the Carleton University micro-fabrication lab. Nitrogen (N_2) and NH_3 gas were obtained from Praxair Canada Inc.

2.1 In-house FGO Synthesis

Two different synthesis methods were used to make FGO. A commercial chemical agent and an in-house hydrothermal process were synthesized using the FGO preparation method. The commercial fluorination agent, XtalFluor-E 2 g of and 2 mL of 2 mg ml^{-1} GO solution were chemically modified by dissolving them in 48% HF solution. The consolidated solution is then boiled at 180 ^{0}C for 2 h.

The reaction was quenched with sodium hydrogen carbonate (5%), washed thoroughly with de-ionized water and sample dried.

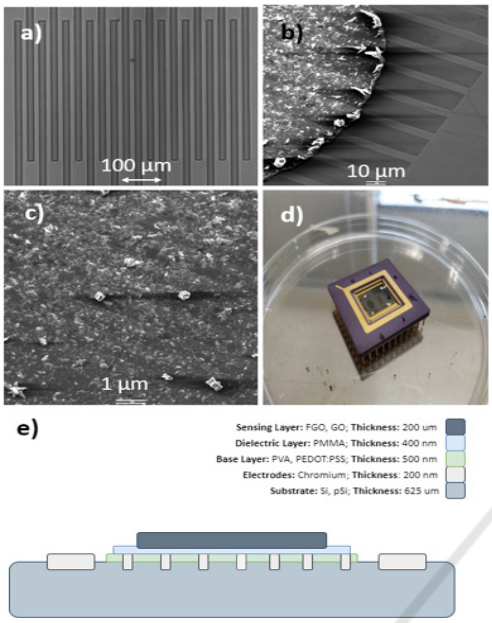

Figure 1: Micrographs showing a) Optical microscope image of IDE chrome structure, b) Scanning Electron Microscope (SEM) image of drop casted FGO film on the IDE structure, c) SEM micrograph showing distribution of FGO micro-particles on sensor surface and, d) a fully packaged FGO NH_3 gas sensor device, e) Device Cross-Sectional diagram.

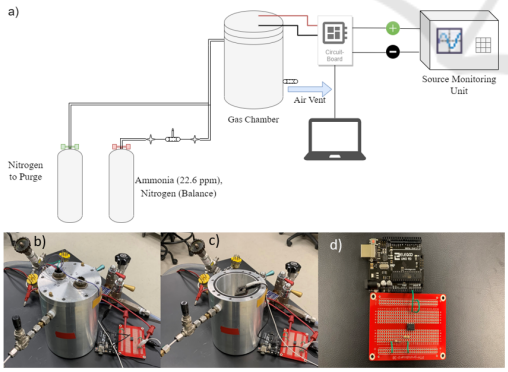

Figure 2: a) Schematic of the experimental setup. b) Closed-lid chamber and c) Open-lid chamber setup. d) Amplifier circuit for voltage monitoring and capture.

A relatively low-cost in-house hydrothermal FGO preparation method was developed and tested. Here, GO (50 mg) was dispersed in 20 ml of deionized water ultrasonically, and 5 ml of HF (49%) was added with moderate stirring. The mixture was stirred on a hot plate at 150 °C for 20 h. The resulting solution was quenched using sodium hydrogen carbonate (5%), centrifuged and washed several times with de-ionized water. The final product was then freeze-dried.

2.2 IDE Chemiresistive Sensor Fabrication

The IDEs used in this experiment were micropatterned using standard photolithography of 200 nm chrome layer, deposited on Si and pSi substrates in Fig. 1a).

The IDE structures on the pSi substrate were layered with PEDOT: PSS (conductive) and PMMA (di-electric). A homogenous suspension of GO and the different samples of FGO (0.2mg/ml) were drop coated using a micro-pipette on each of the different devices (Fig. 1b, c).

The sensor microchip was wire bonded onto a package shown in Fig. 1d), that was then used to connect the device to the circuit for measurements. The packaged sensors were exposed to NH_3 and other target gases for an established period under both controlled and normal environmental conditions at ATM as seen in Figure 2b) and c). The experiments were repeated to verify reproducibility, reversibility, and sensor behaviour.

2.3 Experimental Setup

The initial experimental setup is shown in Figure 2a). NH_3 and N_2 gases were released into the stainless-steel test chamber and used to verify the concept of targeted gas sensing in an ideal, controlled environment. The packaged sensor was placed inside the gas chamber. A vacuum pump was used to achieve a chamber pressure of ≤ 0.00533 kPa (40 mTorr). The ammonia gas cylinder with a rated concentration of 22.6 ppm, was then attached to the chamber with a needle valve to control the flow of gas released into the chamber with added precision. A flow of ammonia gas was released for 3 minutes by opening the needle valve at around 15%. The nitrogen gas was used to dilute the ammonia and return to atmospheric baseline readings. In certain control experiments, a commercial Honeywell Ammonia Gas flow sensor (MIDAS-E-NH3) was introduced in the setup to measure and correlate the ammonia concentration to the response of the chemiresistor gas sensor.

The sensor device was connected in series as the second resistor in a voltage divider circuit to feed the input voltage, V_{in} from the SMU for the instrumentation amplifier *AD 620*. The voltage measurements were then recorded over time.

2.4 Experimental Procedure: Data Capture and Analysis

The data was captured with respect to the voltage of the amplifier V_O over time and was used to characterize the normalized change in resistance defined as |ΔR/R| (%): where ΔR is the resistance change with respect to the baseline resistance R before exposure to ammonia.

The sensing mechanism was exposed to a steady flow of ammonia in a closed environment then extensively verified in an open chamber in an ambient setting to mimic practical health monitoring applications. Responsiveness and selectivity of the devices in these conditions were validated, in significantly lower gas concentrations. Experiments were repeated in an open chamber with ammonia gas flow at concentrations below 2.26 ppm on top of the sensor surface, to mimic exhaled breath sensor response under atmospheric pressure conditions.

2.5 Material Characterization for FGO

Fourier transform infrared spectroscopy (FTIR) is performed on several GO and FGO (XtalFluor) and FGO (In-house) samples using a KBr pellet method, scanning from 400 to 4000 cm^{-1}. Absorption and Transmittance spectra are analyzed to compare efficacies of GO functionalization methods.

The X-ray photoelectron spectroscopy (XPS) data was collected using AlK$_\alpha$ radiation at 1486.69 eV (150 W, 10 mA), charge neutralizer and a delay-line detector (DLD) with three multi-channel plates. Survey spectra are recorded from -5 to 1200 eV at a pass energy of 160 eV (number of sweeps: 2) using an energy step size of 1 eV and a dwell time of 100 ms. High resolution spectra for F1s, O1s, and C1s are recorded in the appropriate regions at a pass energy of 20 eV (number of sweeps: F1s, 15; O1s, 5; C1s, 5) using dwell time of 300 ms and 0.1eVstep size.

Characterization results from the FTIR and XPS are detailed in the results and discussion section.

3 RESULTS AND DISCUSSIONS

3.1 Characterization Results for FGO

Analysis of the obtained spectra for the GO and the FGO showed that the C–O bond at Wavenumber ~1052 cm^{-1} diminishes and is subsequently replaced by another peak at ~1166 cm^{-1}. Based on literature and results obtained previously, the resulting peak indicated the formation of a C-F bond, hence fluorination of the GO. A vibration characterizing a carbonyl group C=O at wavenumber ~1720 cm^{-1}, which is originally present in the GO sample, diminishes upon the fluorination reaction using both methods (HF thermally, and the HF/Xtal Fluor). The shift of wave numbers was also noted for the bond vibration of –C=C-, ~1618 cm^{-1} with a marked decrease in the intensity of transmittance. Intensity of the peaks associated with the carbon oxygen bonds decrease and a strong peak at ~1166 cm^{-1}, corresponding to covalent C–F bond, appears in the FTIR spectrum of FGO (Gong et al., 2012), indicating that oxygen-containing functional groups are replaced by fluorine. The bond C–F (sp^3) vibrates at the wave number ~ 1082 cm^{-1} and is observed in the FGO spectrum. The peak at wavenumber ~2928 Is X=C=Y, where X and Y can be either C or O. C–F formation was obtained from the results of the XPS data analysis. Differences between the GO and FGO decomposition XPS spectra in Fig. 3 a) C1s, b) O1s and c) F1s confirmed fluorination.

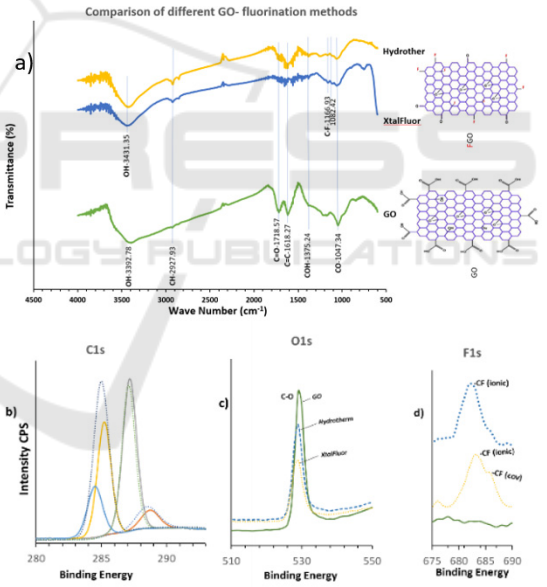

Figure 3: a) FTIR spectra of GO fluorination with XtalFluor and with hydrothermal (Hydrother) fluorination in HF. The GO spectrum is a reference showing the different peaks that are formed due to the fluorination. The two molecular structures of GO and FGO are representative structures, showing likely fluorination positions, b) The XPS figures show the comparison between GO before Fluorination and after Fluorination for C1s, c) O1s and d) F1s. In addition, c) and d) show comparison of the different synthesis products.

Comparison of the XPS C1s spectra decomposition showed characteristic peaks at: C=C, 284 eV, Csp3, Csp2, –CH 285 eV, C–O 287 eV and O–C=O 288 eV. The peak intensities of C–O and C=C/C–C display a significant increase due to the formation of various C-F bonds. This confirmed the reduction of the C=O in the FTIR spectrum and the appearance of the C–F peak. Observed in XPS C1s of the C=O is an increase and shift in the FGO spectrum. F1s spectra Fig. 3d) shows the presence of semi-ionic C–F bonds and the covalent C–F bonds corroborated by the significant increase of C1s, Csp3, Csp2, –CH peak in the FGO spectrum compared to the GO, with no notable increases in C=O and –C–O.

From the experimental results spectra, C–F bond formation was observed in both fluorination processes and that using the in-house method of synthesis would equally facilitate the formation of the FGO–NH_3 complex molecule. A comparison of the inhouse thermal synthesis of FGO and use of the commercial chemical XtalFluor is shown in figure 3c. The depletion and shift of the HC–O at 532 eV was observed as it is consumed in the production of C–F bonds. The graphs in figure 3c), d) also show a comparison of the two FGO synthesis methods products with that of GO, where the appearance of the C–F (ionic) bond is observed at 682 eV and C–F (covalent) bond at 687 eV for both synthesis methods while there is no peak at all for GO. The C–F covalent bonding is noted in the XtalFluor synthesis, suggesting superior fluoride doping, however, the simplicity and high yield of the inhouse thermal process makes it more desirable.

3.2 Substrate Selection for IDEs

A novel component of our chemiresistor sensor is the ability to use a readily available, inert substrate. We used pSi in our tests due to its low cost, non-conductive nature. PEDOT:PSS has a proven conformal contact with textured silicon, and was used as a thick hydrophobic conductive film, with high porosity (Jiang et al., 2018; Vosgueritchian et al., 2012).

We observed that PEDOT:PSS was effective in lowering the baseline resistance from bare pSi at 1.2 MΩ to 133.3 kΩ, however its response to ammonia gas was undesirable (see Fig. 4), and necessitated another coating layer to prevent the interaction between the target molecules and PEDOT:PSS. PMMA was chosen due to its fibrous composition and very low chemical affinity. The thin film stack aids in the retention of gas molecules, possess excellent dielectric properties (Zhang et al., 2014), and therefore proved helpful in trapping analyte molecules and facilitated interaction of FGO with NH_3.

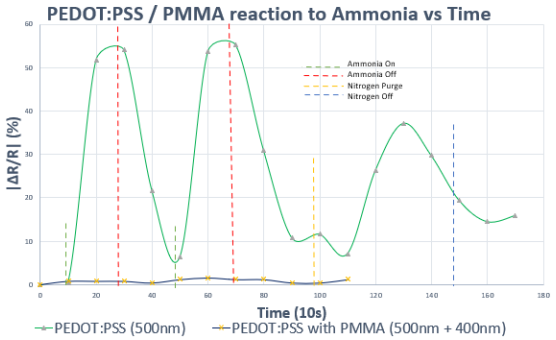

Figure 4: Substrate responsiveness coated with PEDOT:PSS (500 nm), PEDOT:PSS & PMMA (500 nm + 400 nm) with respect to ammonia exposure over time (sampled every 10s).

The results in Fig. 4, confirmed that adding an adequately thick layer of PMMA on to the PEDOT:PSS base layer renders it dormant. Having a high surface to volume ratio also enhanced the effectiveness of PMMA as it covers the layer of PEDOT:PSS and limits interaction with the exposed gas molecules.

3.3 Sensor Performance

The initial transient results of the four tested structures were captured and delineated, as shown in Fig. 5a). The traditional graphene oxide demonstrated no response to the presence of ammonia as expected. All three functionalized graphene oxide sensors were measured in terms of absolute percentage change and demonstrated a visible response to the presence of ammonia. After the nitrogen purge, the voltage output approached nominal readings.

The graphene oxide demonstrated no discernible change in resistance upon initial exposure, whilst the three functionalized sensors all reacted within the first 10 s. The resistance change would continue to rise for the first 90 s of each test, at which point gas concentration then diminished. The two hydrothermally processed FGO sensors had similar maximum resistance changes, with the peaks being at 7.4% for 30% HF and 6.1% for the 49% HF sensors.

The XtalFluor processed sensor demonstrated a larger resistance shift with a peak change of 8.9%. and demonstrated the fastest drop in resistance, indicating quick molecular discharge from the sensing film. In Figure 5a) the 49% FGO (FGO49) had the slowest drop in percent change, indicating

that the stronger affinity causes a retention of ammonia particles.

Following the nitrogen purge, the FGO49 also had the least amount of variation, further indicating its affinity for stronger retention with ammonia particles, while the other sensors dropped rapidly. Within the first minute of turning the vacuum pump back on, all sensors had returned close to the original resistance. The results demonstrate that the functionalization process introduced an electrical sensitivity in the previously unmodified graphene oxide device.

3.3.1 Validation of Sensor Performance

All investigations for sensor performance validation was done using our in-house synthesized FGO. A commercially available ammonia sensor (Honeywell MIDAS-E- NH3) was tested in conjunction with the FGO sensor at atmospheric pressure to calibrate the chemiresistor sensor response. Ammonia was released into the chamber until it reached a concentration of 19 ppm.

The functionalized gas sensor responds to the ammonia within seconds of exposure while the commercial sensor only responds after the concentration has reached 9 ppm. The linear response of the chemiresistive gas sensor peaks at approximately $|\Delta R/R| = 8\%$ at 19 ppm, indicating a sensitivity of 0.42% $\Delta R/R$ per ppm.

Both sensors showed an immediate response to the decreasing ammonia concentration, with the FGO chemiresistive sensor having a slower response. Within five minutes of non-exposure, the chemiresistive sensor returned to its baseline value. The response of the chemiresistive gas sensor is seen to be linearly proportional to the concentration of ammonia on the sensor coating.

Figure 5b) demonstrates the sensor exposed to a flow of an ultra-low concentration (2.26 ppm) of ammonia gas. The peak response was around 8%, and the overall change was a $|\Delta R/R|$ of ~3.54% per ppm. The adjusted scaled percentages corresponded to the same linear response that was modelled from previous experiments conducted in ideal conditions. This data validates that the sensor response remains linear over a broad concentration range and the sensitivity is reproducible for ultra-low concentrations (~ 1-2 ppm).

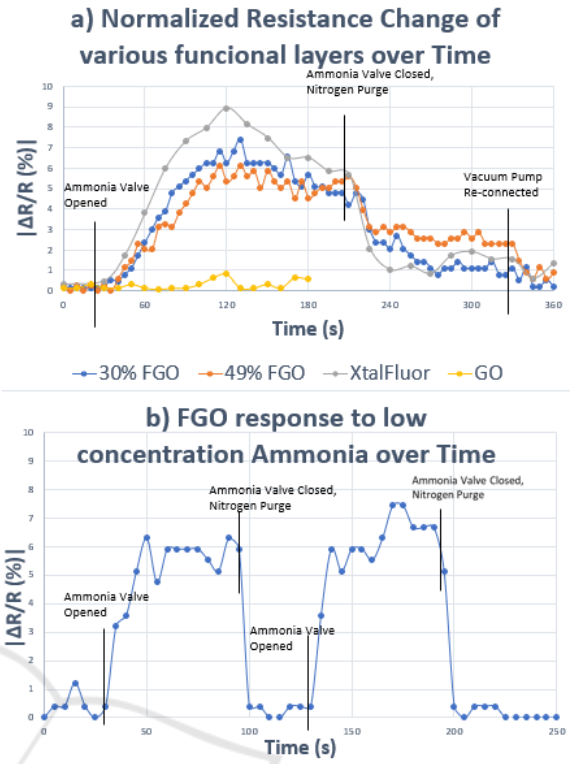

Figure 5: a) Response of FGO (30 and 49%), XtalFlour, and GO to high concentration ammonia. b) Response of FGO to low concentration ammonia.

3.3.2 Multi-analyte Sensing Capabilities of Our FGO Chemiresistive Sensor

The FGO sensor was exposed to acetone to verify its cross-sensitive performance. Acetone possesses enhanced binding mechanisms with FGO. Its chemical features are consistent with previously tested analytes, as interaction with weakly bound fluorine ions change the electronic properties of the sensor. In this case, it provides an opposite, but equivalent response. The experiment was conducted in a controlled environment with both the FGO and GO sensors exposed to acetone in closed, and open lid situations to verify performance under ideal, and ambient conditions.

The acetone was heated on a hot plate at 56 °C and was placed into the sensing chamber. In Fig. 6, device exposure to acetone vapour demonstrated the expected, opposite response. The overall responsiveness to ammonia $|\Delta R/R|$ (%), equal cross-sensitivity and linear correlation of the sensor was predictable and remained unchanged. The trend showed that the peak exposure from the acetone vapour occurred at 20 s.

The change in $|\Delta R/R|$ (%) reached a maximum of 5% for the FGO sensor in a closed chamber. The FGO

sensor in ambient conditions as well as the GO sensor in both open and closed environments demonstrated limited response. The device henceforth proved capable of targeting multiple, opposite analytes, and shows a distinct, predictable trend which can be attributed to the selectivity of the chemiresistor response.

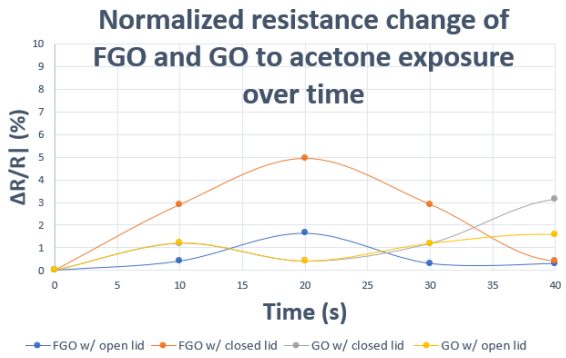

Figure 6: FGO and GO response to acetone.

The change in |ΔR/R| (%) reached a maximum value of 5% for the FGO sensor in a closed chamber. The FGO sensor in ambient conditions as well as the GO sensor in both open and closed environments demonstrated limited response. The device furthermore proved capable of targeting multiple, opposite analytes, and shows a distinct, response which can be attributed to the selectivity of the chemiresistor device at an ultralow concentration range. Since concentration ranges of acetone in exhaled breath of people with diabetes can be as low as ~ 1.8 ppm, the sensor response fits well within the physiological monitoring range.

To further verify the sensing capabilities of the coatings, the FGO and GO coated sensors were exposed to a slow, timed-release of isopropyl alcohol (IPA) and ethanol. Neither the GO nor FGO sensor responded to IPA or ethanol. It furthermore proves to be extremely promising for being highly selective towards specific analytes in ultralow concentrations.

4 CONCLUSIONS

In this work, we achieved ultra-low-level detection (~1-10 ppm) of NH_3 using an in-house synthesized FGO coated chemiresistive gas sensor. The device performance was superior to a commercial electrochemical NH_3 sensor in detection limit, sensitivity, and linearity. The design of these chemiresistor devices can be configured in a way that the sensing layer and substrate are interchangeable, which makes them advantageous. Passivated silicon emulated a low-cost, robust polymer substrate. In the future, these devices will be printed on lower cost substrates, with low production cost. The conductive layers of, PEDOT:PSS and PMMA would provide necessary conductivity and limit interaction with the targeted gas. We demonstrated the miniature footprint of the packaged device which would evolve into a point-of-care, wearable, continuous monitoring exhaled breath sensor. The chemiresistive sensor device was extended to detecting another relevant target gaseous analyte, acetone. Acetone was detected by virtue of a different type of chemical interaction between the FGO and the analyte molecule. Our experiments suggested that the sensor could handle concentrations of acetone in the ~ 1.0 -10 ppm range, which is ideal for physiological monitoring of diabetes. Extensive experimental validation using a commercial gas sensor as control and ultra-low concentration of gaseous analytes validated that our FGO chemiresistive gas sensor has a unique, target specific, transient response that can be easily analysed using simplified techniques, illustrating the versatility of these sensors over traditional electro-chemical sensors. This work furthermore establishes a roadmap to fabricate such sensors on a low-cost polymer surface with configurable sensing layers, to identify presence of multiple gaseous analytes in ultra-low concentration range of 1 – 10 ppm. The small footprint of the device also serves useful for smart wearable type health monitoring applications.

ACKNOWLEDGEMENTS

The authors acknowledge Mr. Brian Kennedy at the KennedyLabs (Ottawa, Canada) for providing graphene and GO samples, and NSERC Canada for the supporting the reported work through the NSERC Engage Grant.

REFERENCES

Yadava, L., et al. (2012). *Detection and sensing mechanism of acetone with modeling using Pd/TiO2/Si structure.* Thin Solid Films, 520(7), 3039–3042.

Sanchez, J.-B., et al. (2006). *A selective gas detection micro-device for monitoring the volatile organic compounds pollution.* Sens. Act. B: Chem., 119(1), 227–233.

Lin, C., et al. (2015*). Evaluation and calibration of Aeroqual series 500 portable gas sensors for accurate*

measurement of ambient ozone and nitrogen dioxide. Atm. Env., 100, 111–116.

Zampolli, S., et al. 2007. *A supramolecular approach to sub-ppb aromatic VOC detection in air*. Chem. Com. 2790–2792.

Majumder, S., et al. (2017). *Wearable Sensors for Remote Health Monitoring.* Sensors (Basel, Switzerland), 17(1), 130.

Zhao, Y. et al. (2020). *A wearable freestanding electrochemical sensing system.* Science Advances, 6(12).

Gargiulo, V., et al. (2020). *Graphene-like layers as promising chemiresistive sensing material for detection of alcohols at low concentration.* Food Re. Intl., Volume 119., May 2019, 99-109

Wang, C., et al. (2010). *Metal Oxide Gas Sensors: Sensitivity and Influencing Factors.* Sensors, 10(3), 2088–2106.

Ponzoni, A. et al. (2017). *Metal Oxide Gas Sensors, a Survey of Selectivity Issues Addressed at the SENSOR Lab, Brescia (Italy).* Sensors, 17(4), 714

Manginell, et al. (1997). *Overview of micromachined platforms for thermal sensing and gas detection*. In V. K. Varadan & P. J. McWhorter (Eds.), Smart Structures and Materials 1997: Smart Electronics and MEMS. SPIE.

Bârsan, N., & Tomescu, A. (1995). *The temperature dependence of the response of SnO2-based gas sensing layers to O2, CH4 and CO.* Sens. Act. B: Chem., 26(1–3), 45–48.

Zhao, W.-J., et al. (2019). *A Low-Temperature Micro Hotplate Gas Sensor Based on AlN Ceramic for Effective Detection of Low Concentration NO2.* Sensors, 19(17), 3719.

Briand, D., et al. (2000). *Design and fabrication of high-temperature micro-hotplates for drop-coated gas sensors.* Sens. Act. B: Chem., 68(1–3), 223–233.

Zaaba, N. I., et al. (2017). *Synthesis of Graphene Oxide using Modified Hummers Method: Solvent Influence.* Procedia Engineering, 184, 469–477.

Huang, X., et al. (2011). *Graphene-Based Materials: Synthesis, Characterization, Properties, and Applications.* Small, 7(14), 1876–1902.

Kavinkumar, T., et al. (2015). *Effect of functional groups on dielectric, optical gas sensing properties of graphene oxide and reduced graphene oxide at room temperature.* RSC Advances, 5(14), 10816–10825.

Park, M.-S., et al. (2016). *NH_3 gas sensing properties of a gas sensor based on fluorinated graphene oxide.* Colloids and Surf. A: Phys. Eng. Asp., 490, 104–109.

Chronopoulos, D. D., et al. (2017). *Chemistry, properties, and applications of fluorographene.* App. Mat. 9, 60–70

Zhao, F.-G., et al. (2014). *Fluorinated graphene: facile solution preparation and tailorable properties by fluorine-content tuning.* J. Mater. Chem. A, 2(23), 8782–8789.

Karlický, F., et al. (2013). *Halogenated Graphenes: Rapidly Growing Family of Graphene Derivatives.* ACS Nano, 7(8), 6434–6464.

Urbanova, V., et al. (2016). *Fluorinated graphenes as advanced biosensors - Effect of fluorine coverage on electron transfer properties and adsorption of biomolecules.* Nanoscale.

Lu, G., et al. (2009). *Reduced graphene oxide for room-temperature gas sensors.* Nano., 20(44), 445502.

Zhu, W., et al. (2019). *Solvent-free preparation of hydrophilic fluorinated graphene oxide modified with amino-groups.* Materials Letters, 237, 1–4.

Huang, X., et al. (2012). *Graphene-based composites.* Chem. Soc. Rev., 41(2), 666–686.

Schedin, F., et al. (2007). *Detection of individual gas molecules adsorbed on graphene.* Nature Materials, 6(9), 652–655.

Kim, Y. H. et al. (2017). *Chemically fluorinated graphene oxide for room temperature ammonia detection at ppb levels.* Jou. Mat. Chem.A, 5(36), 19116–19125.

Gafare, M., et al. (2014). *Detection of ammonia in exhaled breath for clinical diagnosis- A review.* 3RD INTL. CONF. FUND. AND APP. SCI. (ICFAS 2014): Inn. Res. App. Sci.

Xiao, T., et al. (2014). *Highly sensitive and selective acetone sensor based on C-doped WO3 for potential diagnosis of diabetes mellitus.* Sens. Act. B: Chem. 199, 210-219.

Gong, P., et al. (2012). *One-pot sonochemical preparation of fluorographene and selective tuning of its fluorine coverage.* J. Mater. Chem. 22(33), 16950.

Jiang, X., et al. (2018). *High Performance of PEDOT:PSS/n-Si Solar Cells Based on Textured Surface with AgNWs Electrodes.* Nano. Res. Let., 13(1).

Vosgueritchian, M., et al. (2012). *Highly Conductive and Transparent PEDOT:PSS Films with a Fluorosurfactant for Stretchable and Flexible Transparent Electrodes.* Adv. Fun. Mat.

Zhang, H., et al. (2014) *High-sensitivity gas sensors based on arranged polyaniline/PMMA composite fibers.* Sens. Act. A: Phys. 219, 123-127.